The effect of fine scale seabed morphology and texture on the fidelity of SWATH bathymetric sounding data

Dr. J.E. Hughes Clarke (Ocean Mapping Group, University of New Brunswick)

Abstract

Swath bathymetric sonars are capable of near 100% seafloor ensonification. This observation has often led to the assumption that all features on the seafloor will therefore be identified. However, because of the finite dimension of narrow beam sonar footprints, there is a minimum spatial dimension of feature that can be identified. Furthermore, depending on the type of bottom detection algorithm, topographic or textural features below that scale can have misleading effects on the resulting bathymetry.

A model is presented which combines a user specified swath sonar configuration together with an input seabed topographic and textural model. The model then extracts backscattered acoustic intensity and differential phase time series for use in subsequent bottom detection. The model includes the effect of local seabed slope and texture (modeled as a backscatter angular response that can vary spatially). This allows one to input seafloors of known roughness and textural patterns and to predict the resultant resolved morphology.

The application of this model allows one to predict the smallest size of object that can reasonably be seen and also the appearance and distortion of fine scale features on the seabed by the sonar itself. This has critical applications in hydrographic quality control and scientific and engineering mapping projects.

Résumé

Les sonars bathymètriques sont capables d'une couverture du fond de près de 100%. Cette qualité a souvent conduit à l'hypothèse que toutes les caractéristiques du fond de la mer puissent etre identifiés. Toutefois, il y a une limite spatiale pour les caractéristiques qui peuvent être identifiées due à la dimension finie des empreintes des faisceaux. De plus, dépendant du type d'algorithme de détection, des caractéristiques topographiques ou texturales inférieures à cette échelle peuvent avoir des effets trompeurs sur la bathymètrie résultante.

Un modèle qui associe une configuration du sonar spécifique à l'utilisateur avec une entrée des caractéristiqiues topographiques et texturales du fond est présenté. Ce modèle extrait l'intensité acoustique de rétrodiffusion ainsi que les séries temporelle de différence de phase utilisés par la suite pour la détection du fond. Le modéle inclut l'effet de l'inclinaison locale du fond (modélisé par une réponse angulaire de rétrodiffusion qui peut varier spatiallement). Ceci permet d'entrer des fonds de rugosité connue et des tendances texturales et de prédire la morphologie résultante.

L'application de ce modèle permet de prédire la plus petite taille de l'objet qui peut rasonnablement ℘tre vu et aussi l'apparence et distorsion de fines caractéristiques sur le fond de la mer par le sonar lui-meme. Ceci a de critiques applications en contrôle de qualité en hydrographie et en cartographie scientifique.

Introduction

With overlapping swath survey corridors, one might expect to have completely described the morphology of the seafloor. This expectation would only be true under two conditions:

- the swath data completely cover the seafloor
- The bottom detection method used is capable of resolving all length scales.

The first condition is rarely actually met for modern shallow water sonars operating at normal survey speeds (Miller et. al., 1997). The second condition, furthermore, turns out to false and is the focus for this study.

Swath bathymetric sonars are usually presented with a number of qualifications that describe the width of the coverage and the amount of resolution that can be achieved within that coverage. The usual implication is that 100% coverage can be obtained under certain conditions and that, within a specific subset of that coverage, IHO standards are met. In general external sensors are found to limit the angular sector that can be claimed (Hare et al., 1996; Dinn et al., 1997) to meet these standards. The IHO standards (IHO 1987) are currently being modified to specify under what conditions 100% coverage is required (IHO 1997). The resolution, however, within that coverage remains imperfectly defined. Within the area ensonified, the estimate of the shoallest occurring depth is supposed to be accurate to about 1% of the water depth. Using the method of minimum slant range (usually applied to vertically mounted single, broad-beam bottom detection) such a requirement may be achievable (at least within the ensonified footprint.). However, for the more general case of oblique bottom detection (as used in multi, narrow-beam sonars) such a requirement is ambiguous. Must all features on the seafloor be identified to that vertical accuracy? Or does this apply only to features over a certain defined minimum horizontal dimension? Without a specification of this minimum horizontal wavelength it could be argued that no swath sonar could guarantee IHO accuracy.

In the most recent draft of the IHO document (IHO 1997), within the Special and Order 1 standards there are now object detection criteria. For Special surveys, cubic features > 1m must be "detected" and for Order 1 and 2 surveys cubic features greater than 2m (in depths to 40m, 10% of depth beyond) must be detected. Can a specific sonar find (and accurately locate) such a target? What are the controlling factors? Which of the commercially-available products (all of which claim IHO compliance) can meet this requirement?

Aside from the hydrographic requirement lies the needs of the offshore engineer who is interested in describing the fine scale seabed morphology and texture to predict, among other things, the stability of the seabed (Hughes Clarke et al., 1996). For this the engineer wishes to identify the small-scale textural and topographic variations such as the presence or absence of ripple, dunes, boulder fields, and erosion scour features. All these features exist at horizontal scales of a few decimetres to a few metres. At what depths and with what specification sonar can one identify these features (from surface-mounted systems)?

This paper presents first results of a model developed to aid in the understanding and quantification of the spatial resolution achievable with swath sonars. The model is specifically applied to seabed's exhibiting short wavelength (approaching or below the beam spacing in horizontal dimension) topographic and textural variations to try and answer the questions posed.

Note that in this paper the term "texture" is used to describe spatial variations in the backscatter characteristics of the seafloor (patchiness). The textural variations (driven mainly by changes is surficial sediment composition and fine scale surface roughness) are seen as distinct from topographic variations which are due to changes in elevation of the seabed. Strictly there is no real delineation between roughness and topography as both form part of the complete surface roughness spectrum. The delineation between fine scale bottom roughness and topography is arbitrarily set here as the size of grid node used to describe the topography (10-20cm).

Methods

There are two main approaches to quantifying the limiting spatial resolution of swath sonars:

- Repetitive overlapping benchmark surveys over terrain of know physical dimensions.
- Modeling the response of the sonars.

The first approach is ideal as it provides an unambiguous result (e.g. Brissette et al., 1997), but is limited by our generally deficient knowledge of the true detailed morphology and texture of the seafloor. Examples that compare and contrast differing sonars over identical terrain provide an opportunity to assess relative differences in resolution and thus provide a substitute (e.g. Hughes Clarke, 1996, 1997) but these tests are rare. The second approach, however, involves theoretical modeling. If the model can be shown to reproduce existing groundtruth results it may perhaps be extended to predict the sonar performance (or similar, slightly different configurations) on any terrain.

Model Components

The model developed here (synSwath) uses a number of components:

- Sonar:
  - transmit and receive beam-patterns (including all sidelobes)
  - (specified using no. for array length and shading function)
  - no. beams, beam spacing
  - split-aperture separation in wavelengths
  - attenuation coefficient
  - source level with respect to noise level
  - pulse length
  - digitisation rate
  - pulse repetition rate
- Platform:
  - location and elevation
  - Orientation history.
  - advance rate (speed)
- Seafloor
  - specified by minimum cell resolution
  - topography at each node
  - mean backscattered angular response for each node

The sonar operates in a non-refracting homogenous medium of known sound speed. Optionally the presence of a sea-surface reflector can be added to model the effect of multiple echoes.

Derivation of beam intensity and differential phase time series

A multibeam-sonar is broken down into a series of individual beams. Each beam ensonification pattern is modeled by projection of the transmit-receive beam pattern product onto the model seafloor (Fig. 1A, B). The projection allows for the 3D beam patterns, the beam's instantaneous orientation, and the range, depth and relief of the seafloor (Fig. 1 C, E). The projection accounts for local seafloor variations within the beam intensity pattern (Fig. 1 D, F).

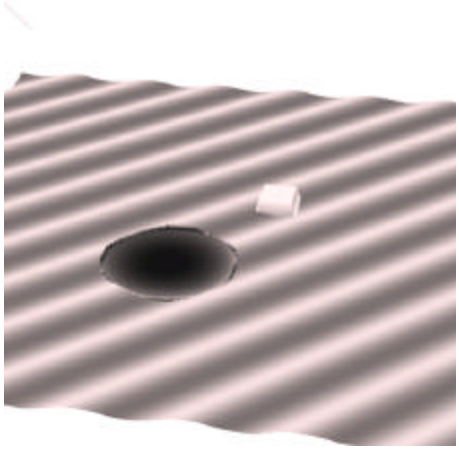

A: oblique view of a model terrain showing: sinusoidal "bedforms", high backscatter block target and low backscatter circular depression.

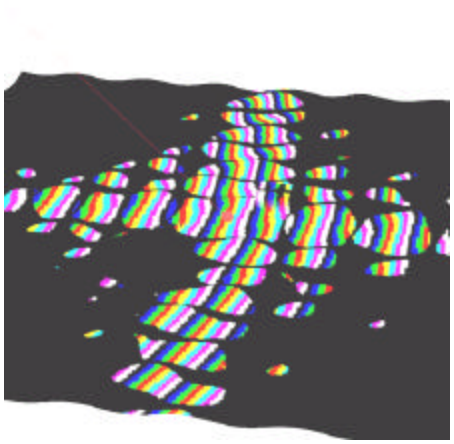

B: seafloor stenciled at the -50dB level showing the propagating annulus. All seafloor within a single color stripe contributes to one backscattered time sample. Source is above and to the left.

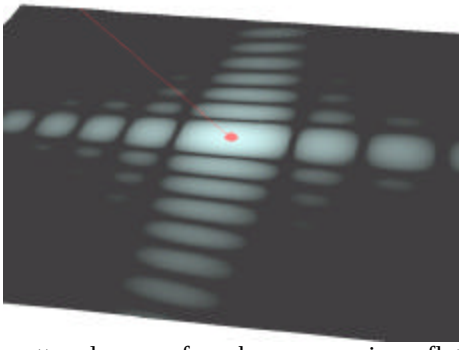

C: backscattered energy from beam assuming a flat and textureless seafloor. Greyscale ranges from white indicating peak backscattered intensity to 50 dB below that level.

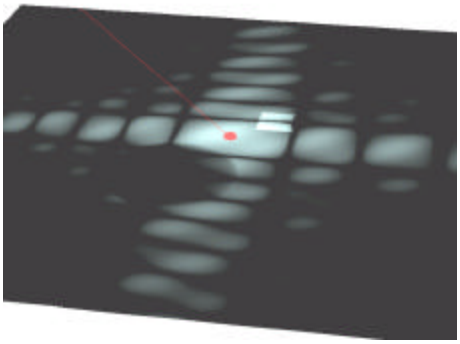

D: same as C but with textural variations.

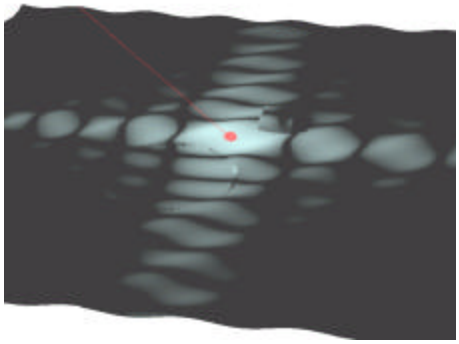

E: same as C but now with topographic variations

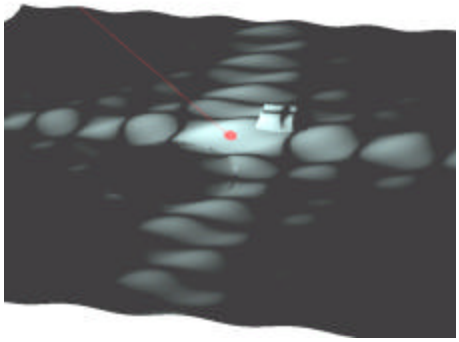

F: same as C but now with both textural and topographic variations.

Figure 1 - Series of figures showing a geometric view of the model beam ensonification pattern superimposed onto a model terrain that can have both topographic and textural variability. The source lies above and to the left with an incidence angle of 45 degrees.

For each node of the model seafloor the following is recorded:

- incident beam intensity (Fig. 1 C, D)
- time of transit (Fig. 1B)
- grazing angle
- (accounting for nodal sea floor slope and azimuth and incident ray vector)
- differential phase for that elevation angle.

The resulting backscatter intensity and differential phase time series is then derived by summing the nodal contributions that lie within the instantaneously ensonified area. This area is constrained by the intersection of the projected beam pattern product and the annulus due to the pulse length at the time of each digitisation step (Fig. 1B). Each nodal contribution is a result of:

- grazing angle
- nodal angular response (mean)
- ensonified intensity at that point.
- Differential phase at that node
- Transmission loss at that slant range.

Because there are only a limited number of nodes within each instantaneously ensonified area, each node quadrilateral is broken down with a 10 by 10 subgrid in which all the parameters are linearly interpolated. This prevent any aliasing effects in the event that the instantaneously ensonified area approaches the size of a single node. The complex sum for all nodes (and subnodes) within that time step is then multiplied by a Rayleigh distributed random variable (with a mean of 1.0) to simulate incoherent scattering. Lastly, a Gaussian-distributed noise vector with random phase is added to the instantaneous backscattered intensity and differential phase vector. The mean noise level can be arbitrarily set.

The result is a time series of the instantaneous backscattered intensity and differential phase for each beam. This process is repeated for all beams within a single swath. After each swath, the sonar is advected forward along a straight path (but free to heave up and down) at the user specified velocity until the next time of transmit, whereupon the whole process is repeated at the new orientation of the sonar at that time.

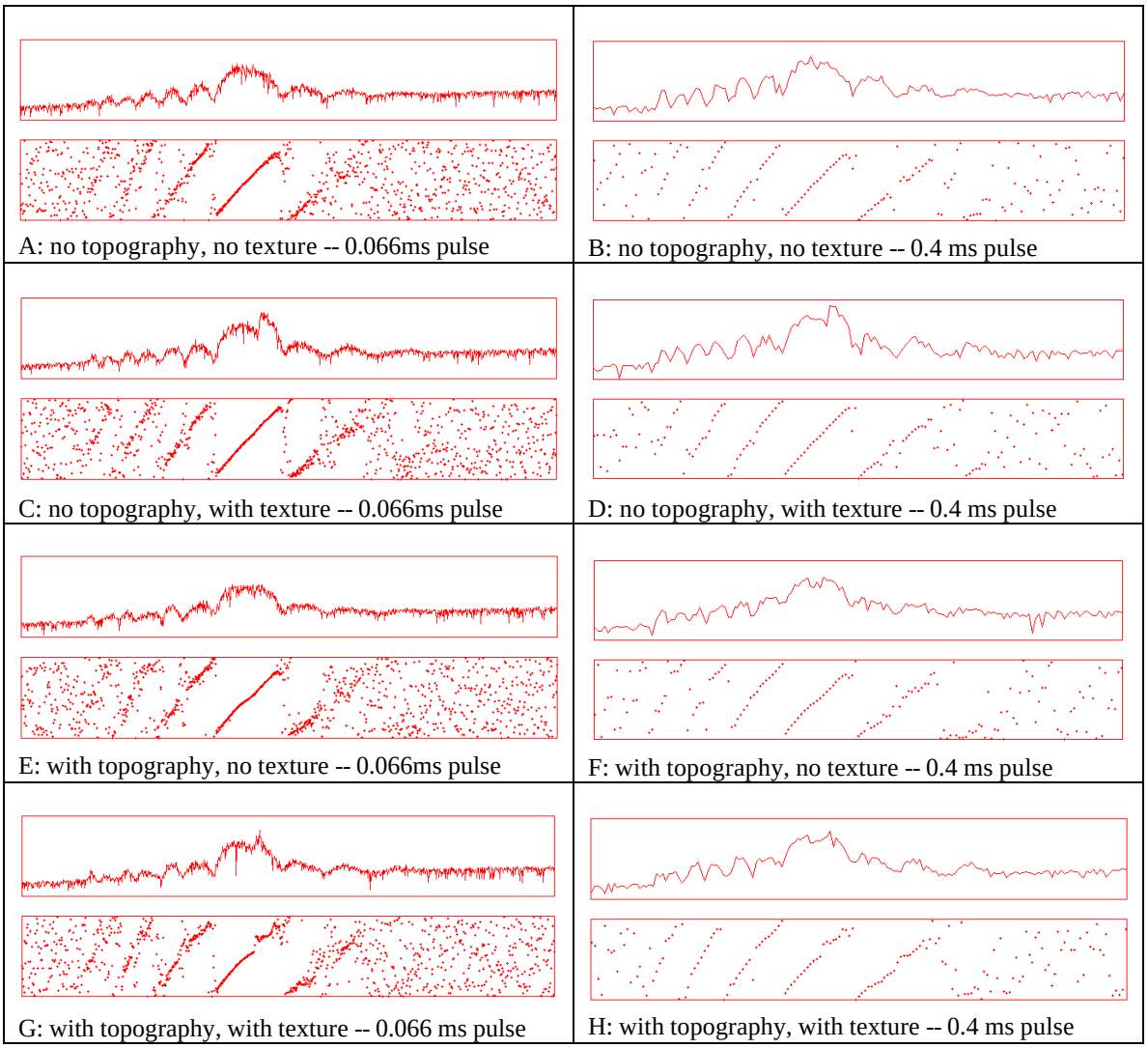

Figure 2 - backscattered intensity and differential phase time series for the seafloor geometry show in Fig. 1. For all figures, a 67 ms time series is shown. The vertical axis for the upper of the two plots (backscattered intensities) ranges over 60 dB. The vertical axis for the lower plot (differential phase) is from -? to + ?. Depth of model 50m., beam incidence angle 45 degrees.

Figure 2 shows model time series results for the geometry used in Figure 1. The beam pattern used had a beam width of 2.4-degrees (at the -3dB level). In order to accentuate the influence of the sidelobe contributions, an unshaded line array model was used. As a result the first sidelobe is only about 13dB below the main lobe. A number of simple observations can be made:

- The backscattered time series consists of a series of pulses as one moves from the inboard sidelobes, through the main lobe to the outboard sidelobes. The main lobe envelope has additional contributions from sidelobes fore-aft .
- As a result of this, the simple envelope pattern seen in Figure 2 A and B can be significantly distorted by spatial variations in the seabed response (due to changes in slope or texture) that occur within the footprint of the main or any of the side lobes.
- A weighted-mean time amplitude detect will be correspondingly biased by these distortions.
- The differential phase time series within the main lobe is distorted by topographic variations within the beam footprint. A least-squares-estimate of this slope will be correspondingly biased by this.

Bottom detection within the time series

For each beam, a bottom detection algorithm may be now be designed and applied. First a gross estimate of the time window that encompasses the time duration of the intersection of the main beam lobe and the seafloor is made. This is done by using a simple peak detection from a running 10 sample average to estimate the centre and thereafter assuming the beam is projected on a flat seafloor to roughly estimate the bounds of likely echo. After the gross detect window has been set, one of two alternate approaches are used:

- weighted mean time : (deMoustier and Alexandrou, 1991) this is done by selecting a signal level above the simulated background noise level. After which the sum total of the acoustic energy above this level is estimated and the point within the detection window at which half the total acoustic energy has arrived is selected as an estimate of the representative two way transit time for this beam.
- zero differential phase crossing: (Hammerstad et al., 1991) this is done by looking at the differential phase time series and fitting a linear or quadratic line to the trend in the data. Depending on the coherence of the phase data, shorter or long time series are used in order to come up with a reasonably robust estimate. For this simulation phase detection is only used when more than 10 samples are available.

These methods are not new, but merely simplified copies of standard bottom detection methods that have been (sparingly) described by several sonar manufacturers. Unfortunately detailed descriptions of specific bottom detection algorithms are rare. DeMoustier (1993) provides one of the few available in the publicly accessible literature. Naturally, because bottom detection is the key to successful swath bathymetry, there is little incentive for commercial developers to describe their methods in detail. More complex approaches are possible including matched filtering (Morgera and Sankar, 1984) or beam deviation indicators (Satriano et. al., 1991). However, for these model simulations a simplistic approach was used to try and reproduce results seen in common shallow water systems.

The end result is an estimate of a series of two-way travel times (TWTT"s) for each ping. Knowing the sonar orientation and position, a series of estimates of the seafloor location and elevation may be made. By compiling these estimates within each swath and then for successive swaths, the sonar model's view of the seafloor can be derived and compared to that input.

EXAMPLE MODEL RUNS

Two examples are presented for a 6-ping sequence over two model terrains. The seafloor used is a rectangle, 80m wide by 26.7m long with an average depth of 40m. The grid node spacing is 13.3 cm. The seafloor was built with two configurations, topographic (Fig. 3A) and textural (Fig. 3E). For each of the seafloor models the sonar was located viewing the seafloor from port side (Fig. 4A). The sonar propagated forward at 12 knots, pinging 6 times, once every 0.12 seconds (Fig. 3B, C, D). The multibeam sonar swath extended from vertical to 60 degrees incidence angle (Fig. 4A). Three sonar models were used:

- 66 1.2 x 1.2-degree beams spaced at 0.9 degrees apart. (Fig. 3D)
- 33 2.4 x 2.4-degree beams spaced at 1.8 degrees apart. (Fig. 3C)
- 16 4.8 x 4.8-degree beams spaced at 3.6 degrees apart. (Fig. 3B)

For all beam patterns used, a cosine squared shading function was used, resulting in a first sidelobe suppression of about -28 dB.

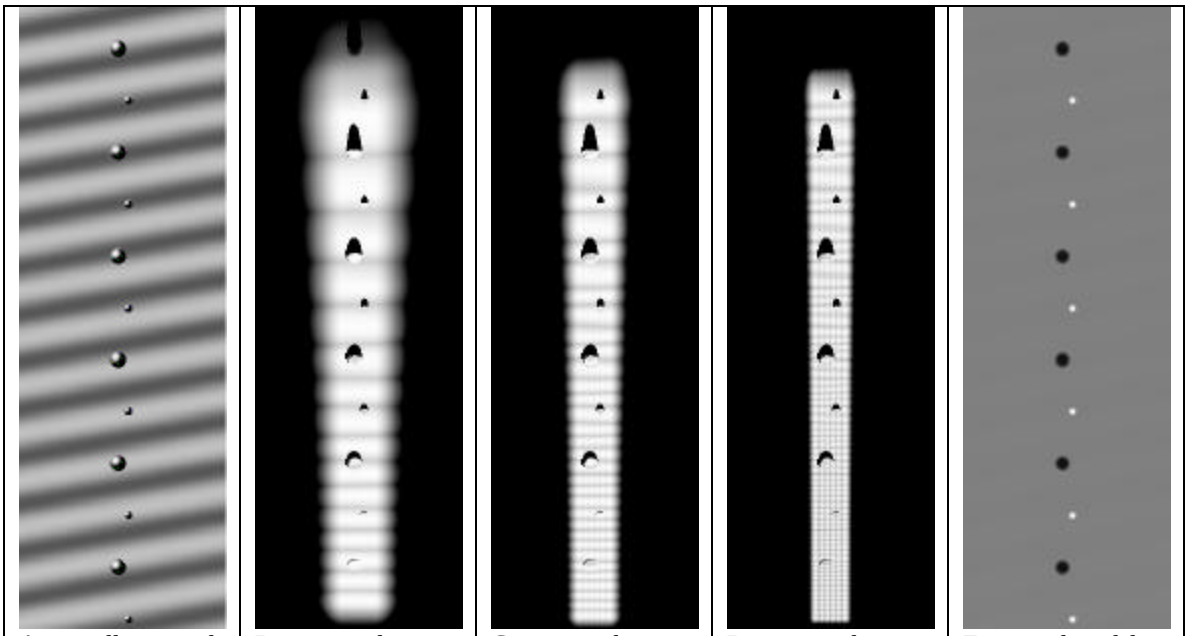

A: sun-illuminated topographic model	B: projected footprints of 6 4.8-degree swaths.	C: projected footprints of 6 2.4-degree swaths.	D: projected footprints of 6 1.2-degree swaths	E: textural model used (with a flat seafloor).

Figure 3 - showing the topographic and textural seafloor model used, together with the projection of the three sonar models used.

(1) Topographic Variations

The model that included topographic variations had the following features:

- mean depth of 40m
- 6m wavelength, 0.5m amplitude sinusoidal pseudo-bedforms (Fig. 4B)
  (strike azimuth at 10 degrees of ships head)
- 2m diameter, 2m high ellipsoidal humps spaced 6.65m apart across track (Fig. 4B).
- 1m diameter , 1m high ellipsoidal humps spaced 6.65m apart across track (Fig. 4B)
  (the two sizes of hump were staggered along track so as to appear in different pings)
- The whole surface has a mean backscatter angular response as shown in Fig. 4C.
  (lambertian for grazing angles below 65 degrees and with an additional 10dB of backscatter toward the specular direction)

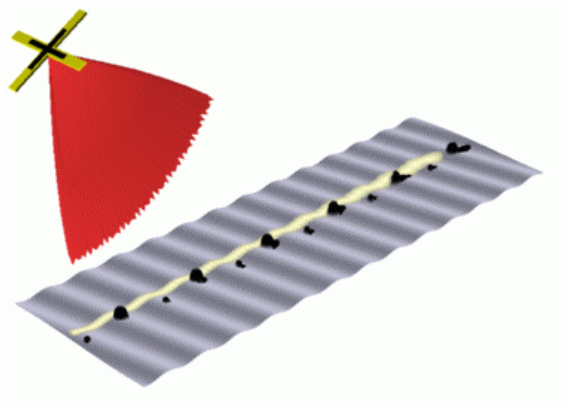

A: 3D view of the imaging geometry

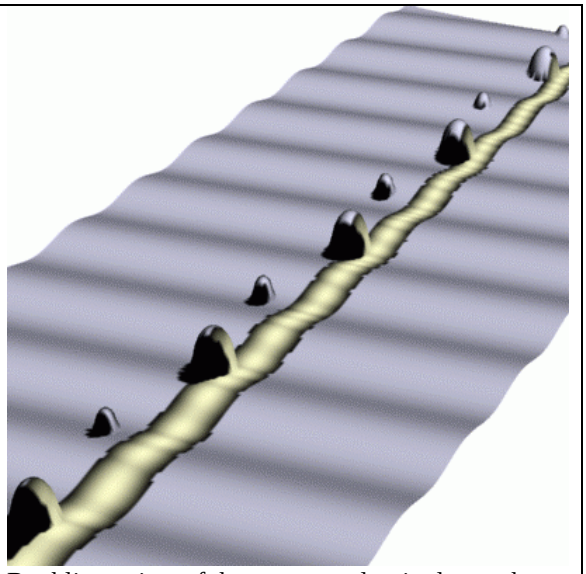

B: oblique view of the targets and a single swath projection. Source in the distance.

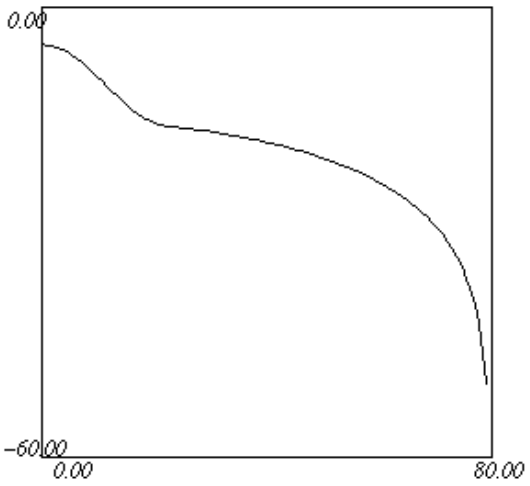

C: mean backscatter angular response used for all the terrain within the topographic model

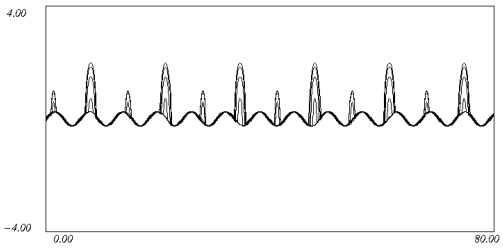

D: 2D profiles through the model terrain along the axis of illumination. This is of the same scale and can be compared directly to the model output profiles in Figures 5 and 6.

Figure 4 - showing the topographic model used, the imaging geometry, the mean angular response and a 2D profile through the terrain imaged. Note the cast shadows that are calculated by the model.

For each beam of each swath of each sonar model, the backscattered intensity and differential phase time series were compiled and bottom detection was attempted. Amplitude detection was attempted for all beams, whereas phase detection was attempted only for those beams that had a minimum of 10 phase samples within the bottom detect window. The six resultant topographic profiles are plotted separately for the three beam widths and the two types of detect (Fig. 5). They can be directly compared to the input topographic model shown in Figure 4D.

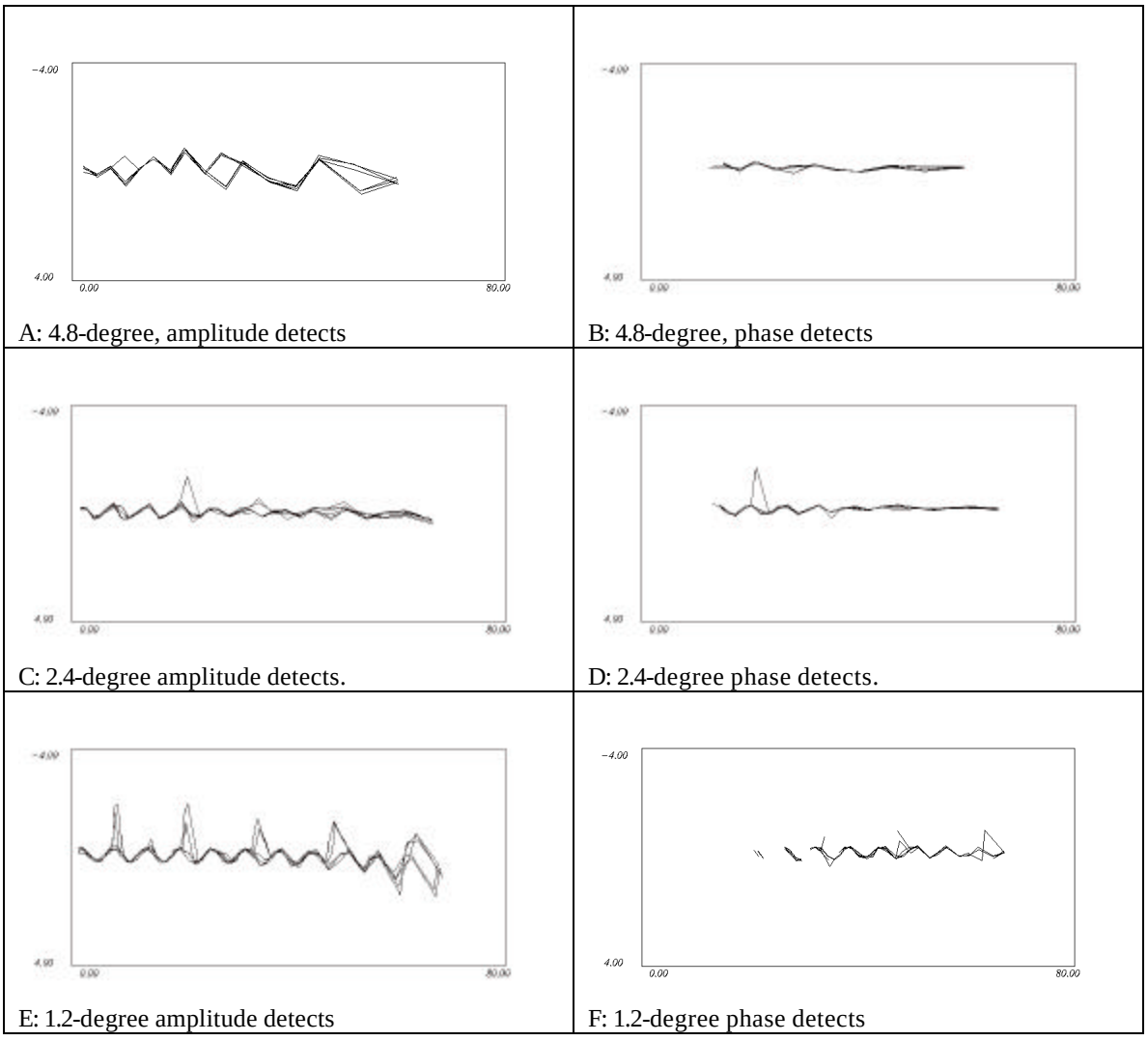

Figure 5 - 6 model beam profiles derived either from amplitude detection (left hand side) or phase detection (right hand side) on the target populated seafloor. For all profiles, the sonar lies to the top left.

(2) Textural Variations

In this case, no topography was introduced into the model. Instead 3 differing seafloor types were used (Fig. 3E). The majority of the seafloor was of the same texture as the previous model. Patches were positioned in which the seafloor mean backscatter response either increased or decreased to a peak value. In the place of the 2m hemispheres, a flat 2m radius patch of **low** backscatter material (angular response of the centre is that of the main terrain depressed by 20dB) was located. In the place of the 1m hemispheres, a flat 1m radius patch of **high** backscatter material (angular response of the centre is that of the main terrain elevated by 20dB) was located.

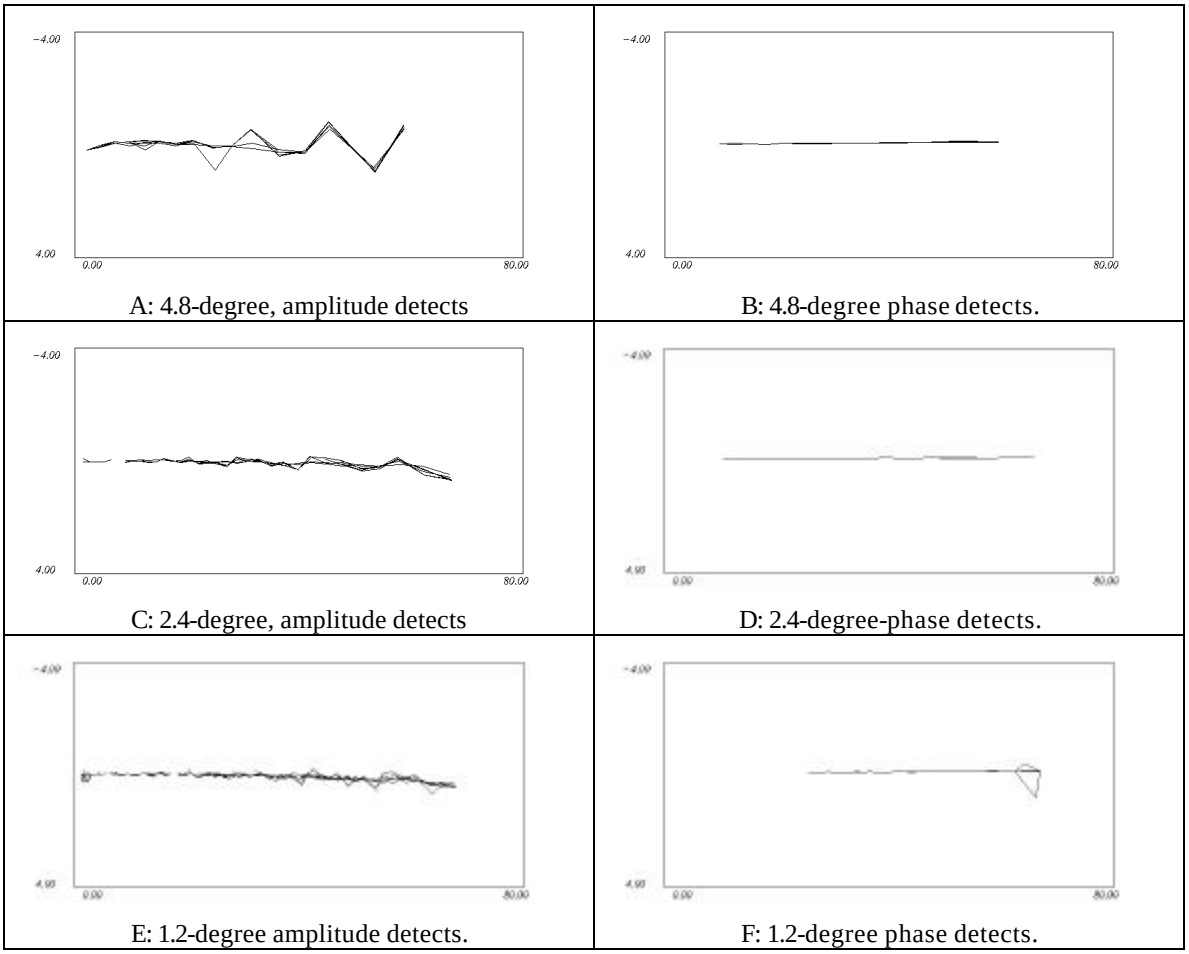

Figure 6 - 6 model beam profiles derived either from amplitude detection (left hand side) or phase detection (right hand side) on the texturally variable seafloor. For all profiles, the sonar lies to the top left.

Discussion

Short Wavelength Topographic Variations

It is clear that the target definition improves with decreasing beam width. Even for the 1.2-degree beams (Fig. 5E) however, the 1m diameter features are not resolved (for the specific conditions of this simulation). The resolution of the 2m targets is highly variable. They are best resolved using amplitude detection (Fig. 5E). This is slightly misleading however, as, by definition, the phase detection will not occur on the shorter echoes of the inward facing targets. The apparent relief of the targets decays with grazing angle, perhaps indicating that the amplitude detection locks onto the near-specular echo from a point on the target that is below the peak. An alternate explanation is that the amplitude detection is biased by the backscatter intensity that arrived from the seabed behind the target (which does not completely block the full beamwidth).

As the beam widths get larger, while relief on the scale of the 2m targets is present, the topography delineated bears little relationship to the real targets (Fig. 5A, B, C, D). Thus the presence of apparent roughness in swath data can be highly misleading. It is notable that the distribution of the target strikes around the true target elevation is far higher than the distribution observed for the surrounding subdued relief. Thus statistics of sonar repeatability, obtained from tests on low relief seafloor should not be taken as indicative of the sonar performance for limiting scale targets.

The delineation of the 6m wavelength sinusoidal features is, in general, better than the discrete targets. In all cases the amplitude detection quality decays with grazing angle. The bedforms are resolved for the entire swath at 1.2-degree beamwidth. (Fig. 5E). The phase detections (Fig. 5F), however, allow better definition of these bedforms at lower grazing angles. For the 2.4-degree beam width (Fig. 5C, D), the beam spacing becomes too wide to resolve the bedforms in the outer part of the swath. And for the 4.8-degree beam spacing (Fig. 5A, B) the bedforms are never resolved.

Short Wavelength Textural Variations

While no topography is actually present in the textural model used, the amplitude detections are clearly biased whenever the beam footprints overlap the anomalies (Fig. 6A,C,E). This results in false topography. If the multibeam sidescan image were examined, one might conceivably believe that the textural features were associated with a topographic anomaly. The phase detects (Fig. 6B,D,F) are notably unaffected by the textural variations as the differential phase is not dependent on intensity (except in that the noise component will increase with decreasing backscatter). The phase result is, however, very dependent on the exact bottom detection algorithm. If the phase sweep is examined only around the region where the amplitude detection is predicted, then a false phase detect will often also result. For the detection algorithm used in this case, the phase solution was allowed to iteratively deviate from the initial amplitude estimate towards regions where a zero crossing actually occurred.

Patchiness on the scale described in the model is quite common. The glaciated terrains of the Canadian continental shelf routinely consist of relict gravel and boulder pavements that are incompletely draped with post-glacial muds. Because of the hummocky terrain of the underlying high backscatter pavement, patchy sediment distributions with backscatter contrasts of as much as 30 dB are intermingled on length scales that are small with respect to the swath width (Hughes Clarke et al., 1997).

Other Possible Simulations

These examples are just two of an infinite variety of simulations that can be run. Other geometry's that could be considered include: equidistant beam spacing; bathymetric sidescan geometry's; lower grazing angle detection; and the effect of varying the along track beam density. Note that without rerunning the projection part of model (the most computationally expensive part) the following parameters may be varied:

- Pulse length
- digitisation rate.
- Bottom detection algorithm
- Noise level and distribution
- Speckle model

The bottom detection algorithm is a critical component. It can be optimised to find or reject spike -like anomalies (generally man made) in favour of more subdued relief (such as naturally occurring sediment transport features). Thus one might use a slightly different algorithm for hydrography than other engineering applications. As the signal to noise level changes, so must the algorithm. Sonar performance for the same shape target will vary greatly, depending on the backscatter contrast between the target and the substrate (e.g. Fig's 1 and 2).

It is important to understand that the model solutions presented here are just one possible realisation for the given conditions. The incoherent scattering (speckle) and noise signal were obtained through the use of a random number generator. If the random number sequence is not reinitialised, the same time series could be recalculated with slightly different speckle and noise characteristics. Thus the same ping can be realised many times allowing one to assess the uncertainty in the bottom detection solution resulting from the noise and speckle.

Conclusions

The model developed here allows one to predict the effect of fine-scale morphologic and textural variations on the fidelity of swath sounding data. The effect of changes in both the sonar configuration (beam widths and spacing, sidelobe suppression and bottom detection algorithms) and the seabed morphology and texture (at scales both large and small with respect to the beam footprint) are graphically demonstrated.

Simulations, performed herein suggest that topographic and textural features that are around or below the beam footprint size will result in misleading fine scale bathymetry. A solitary oblique narrow beam bottom detection should not be assumed to be representative of either the shoalest depth in the ensonified area or the average depth within the area. Rather, because of the aliasing that can occur due to fine scale variations, only through averaging of several closely spaced beams can one come up with a reliable estimate of an average depth. Note that this depth is a filtered view of the seafloor containing information only about wavelengths large with respect to the beam footprint. Targets whose spatial dimension is much larger than the beam footprint should however, be adequately described by swath sonar.

The aim of hydrographic surveying is to ensure the recognition of the shoalest topographic anomalies that might restrict safe passage of marine transport. Now that a minimum required spatial dimension has been defined (IHO, 1997) specific swath sonar configurations will have to be tested to see that they can meet this new requirement. Swath bathymetric surveys increase the likelyhood of identifying a shoal because of the more complete coverage. But, as these model simulations demonstrate, there is a limiting horizontal dimension for target recognition (commonly about 3-20% of the water depth (sonar dependent)) which is always far larger than the often quoted vertical resolution (commonly about 0.2 to 0.8% of the water depth).

Acknowledgements

This research was carried out as part of the Chair in Ocean Mapping at UNB under the sponsorship of the following organizations: Canadian Hydrographic Service, PetroCanada, NSERC, Kongsberg Simrad Mesotech, SeaBeam Instruments, Naval Research Lab., NOAA, Naval Oceanographic Office, Nautronixs, C & C Technologies, MBARI, US Geological Survey, Jacques Whitford-Nortech, James Cook University and International Submarine Engineering.

References

Brissette,M.B., Hughes Clarke,J.E., Bradford,J. and MacGowan,B., 1997, Detecting small seabed targets using a high frequency multibeam sonar: Geometric Models and Test Results: Proc. Oceans 97.

deMoustier, C., 1993, Signal processing for swath bathymetry and concurrent seafloor acoustic imaging: in Acoustic Signal Processing for Ocean Exploration, eds. Moura and Louttie, p.329-354.

DeMoustier, C. and Alexandrou, D., 1991, Angular dependence of 12kHz seafloor acoustic backscatter: J. Acoust. Soc. Am., 90(1), 522-531.

Dinn, D.F., Furlong,A., Loncarevic,B.D., Penny,M. and Dakin,D.T., 1997, Controlling multibeam sonar errors: Sea Technology, v.38, no.8, p.75-80.

Hammerstad, E., Pohner,F., Parthiot,F. and Bennett, J., 1991, Field testing of a new deep water multibeam echo-sounder: Proc. IEEE Oceans'91, 2, 743-749.

Hare,R., Godin,A. and Mayer,L., 1995, Accuracy estimation of Canadian Swath (multibeam) and Sweep (multi-transducer) sounding systems: Canadian Hydrographic Service, internal report.95pp.

Hughes Clarke, J.E., Mayer, L.A. and Wells, D.E., 1996, Shallow-water imaging multibeam sonars: A new tool for investigating seafloor processes in the coastal zone and on the continental shelf: Marine Geophysical Research, v.18, p.607-629.

Hughes Clarke J.E., 1996, A comparison of swath sonar systems demonstrated at the 1996 US/Canada Hydrographic Commission Coastal Multibeam Surveying Course: http://www.omg.unb.ca/~jhc/uschc96/

Hughes Clarke J.E., 1997, A comparison of swath sonar systems demonstrated at the 1997 US/Canada Hydrographic Commission Coastal Multibeam Surveying Course: http://www.omg.unb.ca/~jhc/uschc97/

Hughes Clarke, J.E., Danforth, B.W. and Valentine, P., 1997, Areal Seabed Classification using Backscatter Angular Response at 95 kHz**:** NATO SACLANTCEN Conference Proceedings Series CP-45, High Frequency Acoustics in Shallow Water, p.243-250.

IHO, 1987, International Hydrographic Bureau, Monaco, Accuracy Standards, Special Publication #44, 3rd Edition.

IHO 1997, International Hydrographic Organisation, Standards for Hydrographic Surveys, Special Publication #44, 4th Edition, Draft after 2nd meeting of S-44 WG.

Morgera,S.D. and Sankar,R., 1984, Digital signal processing for precision wide-swath bathymetry: IEEE J. Oceanic Engineering, OE-9(2), p.73-84.

Miller, J., Hughes Clarke, J.E. and Patterson, J., 1997, How Effectively Have You Covered Your Bottom? Hydrographic Journal, no.83, p.3-10.

Satriano,J.H., Smith,L.C. and Ambrose,J.T., 1991, Signal processing for wide swath bathymetric sonars, Proc. IEEE Oceans'91, 1, p.558-561.